processes

MDPI

Article

Simulation Based Approach for High-Throughput Stacking Processes in Battery Production

Alexander Müller [1,*], Muhammed Aydemir [2,*], Christina von Boeselager [3,4], Nils van Ohlen [3,4], Sina Rahlfs [1], Ruben Leithoff [3,4], Klaus Dröder [3,4] and Franz Dietrich [1]

1 Institute of Machine Tools and Factory Management, TU Berlin, 10587 Berlin, Germany; rahlfs@tu-berlin.de (S.R.); f.dietrich@tu-berlin.de (F.D.)
2 Faculty of Engineering, Turkish-German University, 34820 Istanbul, Turkey
3 Institute of Machine Tools and Production Technology, Technische Universität Braunschweig, 38106 Braunschweig, Germany; c.von-boeselager@tu-braunschweig.de (C.v.B.); n.van-ohlen@tu-braunschweig.de (N.v.O.); r.leithoff@tu-braunschweig.de (R.L.); k.droeder@tu-braunschweig.de (K.D.)
4 Battery LabFactory Braunschweig, Technische Universität Braunschweig, 38106 Braunschweig, Germany
* Correspondence: alexander.mueller.1@tu-berlin.de (A.M.); muhammed.aydemir@tau.edu.tr (M.A.)

Abstract: What are the benefits of simulation-driven design and optimization of stacking processes in battery cell production? This question is addressed within the scope of the paper. This work proposes a method to reduce the effort for model-based design and optimization. Based on three case studies which originate from the development of high-speed stacking processes, this paper illustrates how the relevant loads on the intermediate products are determined with the help of the method. Subsequently, it is shown how the specific material models for battery electrodes and separators are identified, created and validated, as well as how process models are created and process limits are identified and optimized. It was possible to prove how process simulations can be used to minimize the effort required to validate developments and to efficiently determine optimized process parameters for a format and material change in a model-based manner. Consequently, more and more model-based processes should be taken into account during development and start-up in the future.

Keywords: production processes; simulation; assembly; battery production

Citation: Müller, A.; Aydemir, M.; von Boeselager, C.; van Ohlen, N.; Rahlfs, S.; Leithoff, R.; Dröder, K.; Dietrich, F. Simulation Based Approach for High-Throughput Stacking Processes in Battery Production. *Processes* **2021**, *9*, 1993. https://doi.org/10.3390/pr9111993

Academic Editor: Andrey Voshkin

Received: 30 September 2021
Accepted: 30 October 2021
Published: 8 November 2021

1. Introduction

Motivation | A production capacity for battery cells of 2000 GWh is predicted for the year 2030, which corresponds to an increase by a factor of 10 compared to today's production capacity [1]. The production of battery cells contributes a significant share to the value creation of an electric vehicle and, in view of the predicted demand, offers great potential for cost reduction through innovations in production technology. One way to reduce costs is to increase efficiency in cell production through higher throughput or lower scrap [2]. Industry and science aim to increase the quality of lithium-ion batteries (LIB) and to reduce costs in manufacturing. Driven by the increasing demand for battery cells and the cost competition, the development of new high-throughput processes comes to the fore of industry and science.

High energy battery cells usually have a prismatic shape (hard case or pouch) [3]. The internal structure of the prismatic shape consists of a stacked electrode–separator composite (ESC) and can be produced by the assembly technologies of winding or stacking. ESC stacking is assigned a central role within cell manufacturing due to its high technical and economic relevance [3,4]. Innovations in production technology contribute significantly to increasing production efficiency in this step, which is cost-driving due to its large number of time-consuming process steps, and is also quality-relevant to avoid contamination.

Inefficiencies are characterized by many non-value-adding downtimes in the material flow of electrodes and separators [5,6]. For example, the throughput of a conventional pick-and-place stacking process is limited due to sequentially executed movements, which always includes downtime. These types of processes are always limited, even with parallelization and increased acceleration of the operated handling movements [6]. In contrast, process substitution through the development of alternative technologies can yield a significant increase in throughput [5,7]. The challenge in process and equipment development of new high-throughput processes is to find a compromise between throughput and product quality, whereby quality in ESC stacking is mainly characterized by the parameters of accuracy and damage-free [8].

The development of new high-throughput stacking processes implies new process and machine parameters that require a deep understanding of interactions to enhance their full potential. However, the development and commissioning process is currently strongly experience-based and often relies on fine-tuning according to "trial-and-error" [9]. During the design phase, a lack of knowledge about these interactions means that reserves are inevitably kept at process level or systems are over-dimensioned, resulting in unused performance potential. In order to make these performance potentials available and to increase material and energy efficiency, product-process interdependencies are currently being derived in the commissioning by means of comprehensive production process monitoring and the subsequent analysis of collected data. With these data and derived interdependencies, material- and format-discrete process limits are being identified [10]. The knowledge gained is used as a basis for the subsequent process and machine optimization, as well as in the process limit determination for new materials or formats. Methods based on production data are already known in the literature [11–14], but mainly focus on electrode production and are always connected with real production equipment and processes. This causes a considerable additional effort. The identification and utilization of these performance potentials by using experimental procedures are associated with a high level of effort in development and commissioning. In addition, the significant material waste [4], caused by the experimental approach, is a major cost factor when introducing new cell formats and materials due to the proportionately high material costs [2] of total production costs [15,16].

Aside from experimental methods, digital tools such as simulations have already been successfully used in related domains of production engineering to support the transition from the design phase to series production [17–20]. The increasing availability of digital tools and computing power has created new opportunities to predict process and machine parameters as well as interactions during the development process, without significantly increasing the associated development effort [20]. These simulation-based approaches, which have already been used successfully, show great potential for application in the development and commissioning of new stacking processes for ESC assembly.

State of research | In addition to various multi-physical models for simulating the temperature behavior during charging and discharging of a battery, the current state of research shows many approaches for the characterization and modelling with a strong focus on the prediction of the material behavior in case of a crash [21]. To simulate these mechanical loads and predict the deformation behavior, finite element analysis (FEA) is mostly used. The approach in development and subsequent commissioning of new high-throughput processes is characterized by experimental methods. Westermeier presented a method for quality-oriented analysis on the example of battery cell production [22]. This method aims at identifying and quantifying interactions through experimental analyses, while the potential of simulation-based analyses in the production of LIB is pointed out. As an example, Weinmann et al. investigates interactions for the feeding and alignment of web-shaped electrodes and the positioning of cut-to-size electrode sheets using the Coil2Stack process as an experimental and simulation-based example and derives process limits [23].

However, FEM simulations are not commonly applied. Different tools are used in the characterization and modelling of battery materials, which are generally categorized to the **micro**, **meso**, **macro** and **system scales** [21]:

- On the **micro scale**, there are research activities at the particle level using the discrete-element-method (DEM) to investigate the change in volume, deformations and particle fractures during the intercalation of lithium-ions. Sangrós Giménez et al. developed a DEM contact model to describe the elastoplastic behavior of the connection between the ingredients of the electrode coating to analyze the fracture under different simulated stress conditions [24].
- At the **meso scale**, properties of individual elements (anodes, cathodes and separators) are investigated as single homogeneous layers through finite element analysis. On the meso scale, Avdeev et al. investigated the mechanical properties of polymer-based separators and observed a strain-rate dependent material behavior [25]. The investigated separator showed a higher stiffness when the strain rate was increased. The investigations from the state of the art and research have shown that separators are characterized as visco-elastic materials with anisotropic material behavior, but in most cases, they are represented in a simplified way via isotropic linear-elastic or visco-elastic material models.
- In the case of the electrode, investigations primarily consider the interactions of specific loads in the context of the electrochemical performance. For example, Zhu et al. investigated the mechanical degradation of electrodes under electrochemical–mechanical conditions with the help of a homogeneous layered electrode model and a finite element software [26]. Mooy investigated different load cases on the electrode caused by different handling processes to align electrodes [6].
- The **macro scale** investigates the ESC up to complete battery cells including electrolyte and housing. A distinction is made between the simplified representation as a homogeneous material and the detailed heterogeneous representation of the individual elements considering multi-layer interactions. This research field contains various investigations on the characterization of the mechanical properties of electrodes and separators. Kermani and Sahraei give an overview of previous activities on experimental characterization and numerical simulation by using FEA [27].
- The **system scale** is used to investigate the structural properties at battery module or system level. Thomitzek et al. investigate the effects of quality fluctuations of individual processes on the battery cell [14]. In addition to the individual process, the effects on the battery cell through the subsequent processes are considered. Accordingly, intermediate product properties are analyzed in coupled process simulations in order to coordinate the individual processes and to obtain the best possible product quality. The production processes were described by mathematical and empirical models, whereby the battery cell was simulated by the widely used pseudo-two-dimensional (P2D) model [28]. The knowledge gained from these simulations subsequently enabled the optimal dimensioning of these processes and revealed process limits [14]. Although a general approach was developed, the simulation of the production process was limited to electrode production with a special focus on calendaring.

In summary, the characterization and modelling of electrodes and separators is well investigated by the current state of the art and research, although most activities focus on simulating the crash behavior of the materials and almost no reference to production engineering is apparent. However, there are already some new approaches for simulation of sub-processes in electrode production. In particular, the simulation techniques, computer fluid dynamics (CFD) and DEM [24,29,30], are used for the coating and drying processes within electrode production. DEM is also used to investigate the mechanical behavior of electrodes during calendaring [31,32]. While modelling the sub-processes of electrode manufacturing has been investigated for several years, simulation-based approaches for process and equipment development for ESCS-stacking have recently emerged as an investigative aspect of recently launched research projects.

In the context of the simulation-based design of an ESC stacking, simulative investigations of interactions between material properties and process have to be carried out for individual elements on the mesoscale and for ESC on the macroscale.

Need for action | It was shown that there is a significant market demand for high-throughput stacking processes. Simulation tools are available to model and digitally design such processes and machines. However, in the past, strongly iterative procedures have been used to develop and commission new types of stacking processes. There are also no known approaches enabling the creation of a target-oriented ESC stacking process model, which uses an optimized material model for the simulation of the handling process. The necessity is characterized by the fact that, especially in the case of format and material changes, a high amount of cost is incurred when all parameters have to be determined and the process has to be optimized through iterative procedures.

In order to keep the effort as low as possible, an approach is needed in which the development and commissioning of stacking processes is carried out in a simulation-based environment. The aim should be to create application-specific material models to identify the best possible process windows in which damage-free handling of the battery materials is possible. Accordingly, it is necessary to pre-analyze the predominant loads of the applications on the product and to select the material model accordingly. With the help of a simulation-based approach, it will be possible to react quickly and without additional effort for new material compositions and format changes. As a result, there is the potential to allow a short set-up time for the production plant when a product change is scheduled in cell production.

2. Materials and Methods

Based on the V-model, according to the guideline 2206 of the Association of German Engineers [33], a procedure similar to the waterfall model is proposed in Figure 1, which is structured in six individual phases; the first three steps increase the level of granularity, while the last three steps decrease the level of granularity. The model starts at the process level of ESC stacking, which is further detailed and specified to individual material parameters. Furthermore, intermediate validation steps are implemented to secure the critical parameters of the simulation. An additional benefit of the proposed approach compared to the V-model is its targeted and efficient procedure for simulation-based format- and material-specific process design and process limit identification.

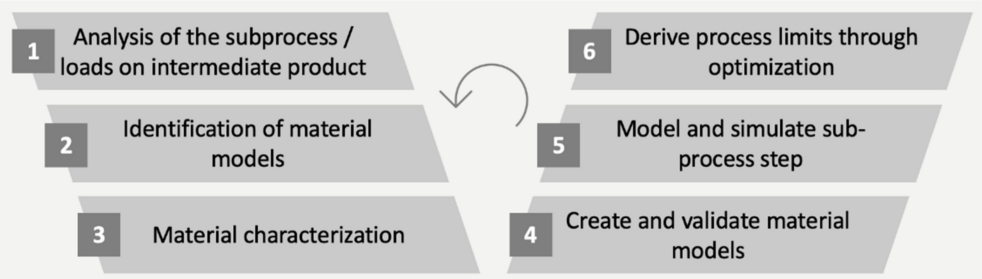

Figure 1. Approach for simulation-based design validation of production processes in cell manufacturing.

1. Step—Process analysis/loads on intermediate products | In the first step, the sub-process of cell assembly is analyzed with regard to its loads occurring on the intermediate product, i.e., the battery materials (electrodes, separator and binder). Depending on the complexity of the stacking process, there may only be a few and obvious loads that act on the intermediate product and can therefore be analyzed easily and assigned to the sub-process accordingly. As an example, in a pick-and-place operation with an area suction gripper, a full-area negative pressure on the electrode represents the primary load, and the flaking behavior of the coating must be considered. However, it is also possible that a very complex dynamic and kinematic handling and assembly process occurs during the cell assembly of the specific ESC stacking process. An example of this is a free-flying phase of the electrode during handling/transport, in which the limp foil can strike somewhere with its leading edges or buckling can occur due to insufficient detention during synchronized

parallel handling. Accordingly, it is recommended to divide the new or adapted ESC stacking process in detail regarding its functional structure, to analyze each individual function and examine the interfaces of the individual connected functions.

2. Step—Identification of material models | For the model-based determination of process limits in the development and commissioning of processes and machines for ESC assembly, the idealization of material behavior represents a main challenge. On the one hand, material models and simulations must consider specific material properties, such as low material thickness, high ductility and material mechanisms such as anisotropy to identify interactions between material and process loads. On the other hand, the determination of material parameters, development of material model and realization of simulation must show an advantage regarding costs and quality in comparison to the purely experimental approach for development and commissioning. For the development of the material model, the material behavior, which naturally has a non-linear characteristic, is idealized in order to consider only certain failure-relevant effects that are important for the analysis and, thus, reduce the effort in the material model's development. Generally known failure-relevant effects are described in Stommel et al. [34].

In classical pick-and-place ESC stacking, electrodes and separators are usually not allowed to suffer any plastic deformation, whereas the goal in z-folded ESC stacking is the plastic deformation of the separator at the folding position. This simple consideration at the level of partial functions shows that different material models have to be used for different loading conditions. For an idealization, material models are to be used which are able to represent elastic, plastic and viscous material behavior. In order not to increase the effort of the approach, it should be carefully considered which characteristic mechanical behavior must be represented by the material model, and which can be neglected. Therefore, the partial function from the process analysis of the first step specifies which characteristic behavior must be represented by the material model for simulation. In this context, the material characterizations that are necessary to create the material models must be carried out in the following third step.

3. Step—Material characterization | Depending on the experience of the user, key figures and datasets from known material databases can be utilized for the material characterization. However, it is advisable to collect the data for the material models on a sample-specific or batch-specific basis, as there exist significant differences in the mechanical behavior of manufacturing types and battery materials.

After determining the characteristic loads in the previous steps, the corresponding material tests have to be carried out according to the selected material model in order to generate the associated data for characterization. Depending on the application, a distinction must be made as to whether the simulation is in the micro, meso, macro or system scale, and the idealized characteristic values for the material models must be generated accordingly. The selection is usually related to the accuracy of the damage that is represented by the simulation. Therefore, in the micro area, a high-resolution characterization method such as nano-indentation is used to generate reproducible key figures at the micro-level and to investigate damage cases, such as the chipping of coating components of electrodes. In contrast, coarser material tests such as uniaxial tensile tests, which can describe the behavior sufficiently, are carried out in the handling processes of battery materials at the macro level.

As deformations and stresses on the product are usually analyzed in the process simulation, it is crucial to characterize the Young's modulus as a function of the loading direction. Depending on the specification and the required accuracy, it may also be necessary to identify additional material characteristics, such as the strain-dependent Poisson's Ratio, the adhesion strength, the impact edge strength, the surface hardness or the bending stiffness. Reference is made to the existing literature on the already developed approaches of characterizing material tests for face pull-off test [24,35], nano-indentation [24,36] and the bending test [36]. However, two new characterization procedures are presented in the evaluation part of the approach for case studies.

4. Step—Create and validate material models | After completion of all required physical material characterization tests in step three, the material models are created and validated in the fourth step. The validation includes, on the one hand, the simulation of the selected material tests and, on the other hand, the integration of the empirically collected data into the material model.

For the simulation of any type of material test, the material samples, boundary conditions and loads must be modelled and defined for the validation. Additionally, depending on the post-processor, the sensors to be defined in advance must be implemented in the test routine in order to generate simulated measured values, which are used to compare and validate the empirical and simulated data.

After the sample has been geometrically modelled, a specific material model is assigned. Depending on the software used, various material models are usually available as a basis. Depending on which material models were identified in the second step, certain key figures, such as the direction-dependent Young's modulus, the density, the Poisson's ratio and/or stress-strain curves, must be integrated. With the help of these parameters, specific material models can be created, which are assigned to the modelled sample.

For validation, the simulation of the experimental material tests is then carried out with the different material models. Afterwards, the simulation results and the experimental data are compared and the material model with best agreement is identified.

Subsequently, it is possible to simulate more complex loads in the stacking process with the identified material model of battery materials and to design them accordingly, since the loads that are applied to the intermediate product are mapped realistically.

5. Step—Model and simulate sub-process | In the fifth step of the approach, the simulation model for the ESC stacking process is created. Depending on the application, the level of detail of the model varies. If, for example, a completely new stacking process is developed without any previous knowledge, the model will primarily represent the basic functionality in order to provide a basic proof-of-concept. However, if the readiness level of the process is already advanced and the throughput of the system has to be increased, or a change of material or format requires new equipment that has to be specifically designed, the level of detail of the simulation should be much more detailed.

If a new stacking process has to be simulated, it should be considered that no a priori knowledge is available and can be utilized. Accordingly, the range of parameter values is very wide in relation to a parametrized and tested simulation. In context, this means that a very robust basic configuration should be modelled as simply as possible and contains the essential functions. As soon as the first basic model converges reliably, the level of detail can be increased further, until all necessary physically influenceable phenomena have been included in the simulation.

Based on experience, the entire stacking process is usually very complex and difficult to represent with just one model. It is therefore recommended to subdivide the ESC stacking process regarding its functional components and initially investigate the characteristic sub-process steps individually. When modelling the individual sub-process steps, the results from the independent simulations are then transferred step-by-step, whereby the entire stacking process can be represented as a unit.

Depending on the computing power, it must be considered which level of detail provides a remarkable benefit and how much time a simulation should take, at most. In general, it should be mentioned that a computing time-efficient simulation model of the stacking process should always be aimed at investigating new configurations as well as format and material changes without great effort. Accordingly, it is recommended to use a multi-level detail expansion of the model and to stop at the level of detail at which the target parameters of the simulation converge to a sufficient accuracy. A computationally efficient simulation also builds the basis for the optional sixth and final step of the approach, where optimization takes place.

6. Step—Derive process limits through optimization | The sixth step of the approach is optional. Depending on the application, it is sometimes sufficient to test and

validate basic functions by simulation and to carry out further improvements on the real system. However, if the process is very complex and the correlation of the parameters is not comprehensible because there are too many dimensions with nonlinear correlations, it is advisable to carry out a customized optimization.

If an optimization is to be considered within the scope of the process design, it should be noted that the model of the stacking process should be parametrically associative [37]. Accordingly, a sensitivity study can be used to identify the value range of the parameters that need to be optimized with regard to the target function. In the stacking process, the target function should consider the economic parameters of the stacking process, such as the throughput time, but also contain boundary conditions, such as the permissible loads from the material characterization. The boundary conditions ensure, for instance, that the material is handled damage-free.

With the aid of the optimization, it is possible to geometrically design the equipment and/or to determine optimal process parameters, which represent the suitable format- and material-specific setup. In order to fully exploit the process limits during the simulation, it is important to know the relevant parameters (boundary conditions, load assumptions, material models) as precisely as possible to avoid any limiting parameter value ranges caused by lack of knowledge and fear factors in the context of optimization.

3. Results

Alternative stacking processes for pouch cells are currently being increasingly developed because established stacking systems represent a bottleneck for the high-throughput ESC production. In this chapter, two selected projects in the field of high-throughput stacking of lithium-ion batteries (HoLiB and KontiBat) are used to demonstrate the potential of model-based simulations for the confident design and commissioning of production processes in cell manufacturing.

First, in the HoLiB stacking process, the handling of the electrode in the separating and stacking sub-processes is specifically addressed, and the way in which model-based process simulations can be used to design and determine robust process limits is shown. Subsequently, the handling of the separator in the KontiBat stacking process is presented, whereby model-based simulations were also used for the design of the sub-processes.

3.1. HoLiB–High Throughput Processes for the Production of Lithium Ion Batteries

3.1.1. General Process Description

The HoLiB process is illustrated in Figure 2 and includes technologies for the process steps of cutting, handling, stacking and welding within cell assembly [38]. The chosen technologies aim to accelerate the cell assembly process. For the laser cutting process, the laser beam passes an optical element before hitting the electrode. This optical element forms the laser beam. This leads to a line-shaped cutting contour on the electrode rather than a laser spot. Consequently, the laser can cut a greater contour at the same time. After cutting, the electrodes are fed into a continuously rotating paddle wheel via a conveyor. The paddle wheel serves as the central handling unit of the process, decelerating and buffering the electrodes while transporting them to the release magazine. Finally, an end stop casts off the electrodes and they fall into the magazines where the positioning and orientation of the electrodes in the stack takes place. As a final step of the process, the stack is contacted via laser welding process.

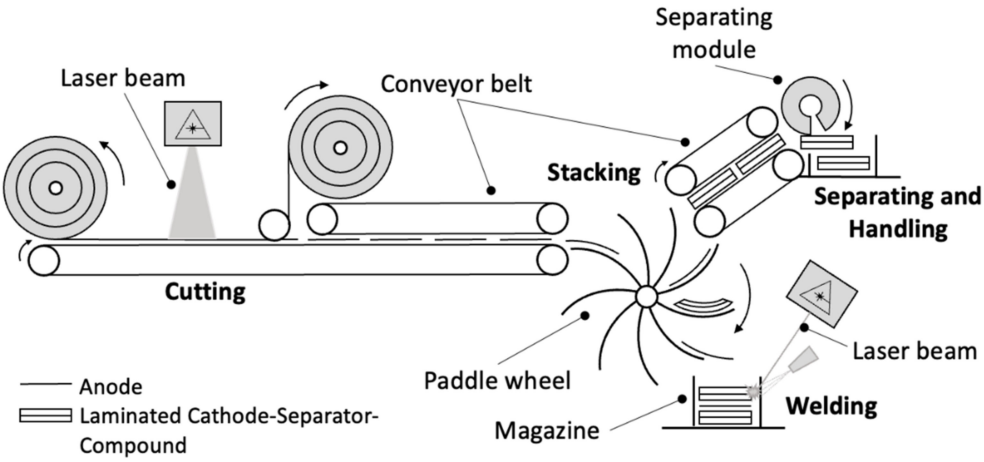

Figure 2. Architecture of the stacking process in the research project HoLiB.

3.1.2. Reasons for Simulation-Based Process Modelling

The handing process in the separation module and the paddle wheel do not apparently represent a major development challenge at first glance, because they are comparable techniques from the paper industry. The difference between electrode production and the paper industry is the intermediate product to be handled, which is limp and consists of a multi-layer composite. Frictional forces on the sensitive surface of the electrode are extremely critical. The electrode can delaminate or its coating can abrade. For these reasons, it is appropriate to use a simulation of the sub-processes to gain specific knowledge about unknown loading effects during handling and to use this knowledge in the design, parameterization and control.

Accordingly, a simulation of the separation process can be used to specifically analyze the deformations in each sub-step of the process. The aim is to detect potential collisions between the deformed electrode and the system during the process and to avoid them through simulated process studies and specific design adjustments. These collisions occur unexpectedly due to the limp behavior of the electrode.

Soft sensors can also be trained with the help of simulation, which are able to derive non-measurable variables that can be used to control and regulate the process or for quality assurance. An example of this is a critical deformation of the electrode that must not be exceeded during separation. The place where the deformation occurs cannot be reached by physical sensors, but it is possible to place a sensor somewhat downstream. With the help of the downstream sensor and the simulation model, the critical deformation or another fault can be detected, for example, because the correlations between the original location and the measuring point are analyzed in the simulation and the correlation is obtained via a soft sensor. With the help of the simulation, it is therefore possible to detect rejects or to correct faulty poses that cannot be measured directly.

In the case of the paddle wheel, a large number of variables exist for the design of the exact shape of the paddlewheel. In order to avoid experimental investigation of countless variants, a simulation is used to determine which parameters have a decisive influence on the stacking process. Through correlation analysis, it is possible to carry out a targeted design study to generate the best possible initial design, to parameterize the novel process for start-up and to define its process window in advance.

Particularly the functional production process window can be determined with the help of simulations for new formats or new materials parallel to product development and can be used directly for the parameterization during the renewed commissioning and start-up of the system.

3.1.3. Disadvantages of an Empirical Approach

The separating and stacking process are innovative processes that are designed for the first time. For this reason, there is no previous knowledge available, and therefore the purely empirical approach would be associated with a high level of effort and correspondingly high costs. The high effort comes from the necessary adjustments of previously unknown problems and effects, which are only identified in the stage of prototyping. As a result, a model-based development approach was pursued for both processes, with the help of which various configurations and sub-processes can be specifically selected and designed through simulations.

Furthermore, especially in the research area, new materials are usually available in small batches. Consequently, an experimental investigation of all possible parameter combinations is not always possible. By using simulations, various parameter combinations can be investigated with the help of characterised materials. In addition, simulations can also be used to determine specific requirements regarding the mechanical specifications of the electrodes in order to achieve the envisaged throughput targets. An example of this is the minimum bending stiffness of the electrode sheets, which contributes to the maximum process speed that can be achieved during handling.

3.1.4. HoLiB—Separating Module

In the following, the proposed method from chapter 2 is applied and explained step by step for the design of the components of the separating process. It has to be pointed out that the approach is always specific, and therefore only the essential loads are taken into account in the design. Accordingly, the results of the method will differ in the contents of the separating module and the paddle wheel.

1. Step—Process analysis/loads on intermediate products | A limiting sub-process of the HoLiB apparatus is the separating module, which separates the single electrodes out of a stack from a magazine with a rotating low-pressure vacuum-suction gripper and accelerates them to the needed web-velocity, as shown in Figure 3.

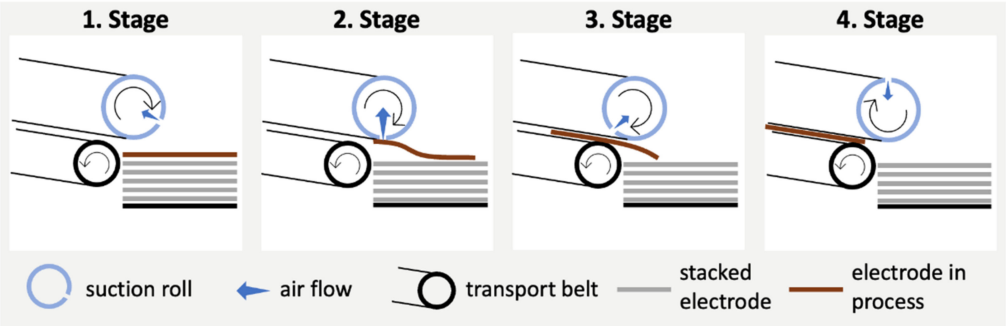

Figure 3. Separating sequence of an electrode from the separating module.

The main challenge of the separating module is that the apparatus has to work as fast as possible to optimize the throughput, but at the same time, the pre-products of the electrode sheets have to be handled as softly as possible to avoid any kind of damage through the handling process. Through these circumstances, the pre-product loads have to be analyzed on each separation sequence to optimize the gripper and other utilities of the machine for an optimized damage-free handling process.

The separating sequence consists of four stages:

In the first stage, the suction roll rotates and orients its suction area perpendicular to the electrode's surface and generates a negative pressure field on it. At this stage, the electrode is not moving and lays still on the stack of electrodes in a magazine, so there exist no resulting loads from the separating module which could damage the pre-product.

In the second stage, the suction roll stands still, the negative pressure field begins to grow and the forces on the surface of the electrode grow larger than the weight force.

At this specific point, the electrode sheet begins to lift and to deform its original shape. Subsequently to this lift-point, the electrode accelerates upwards until the suction area is reached and the nozzle is sealed through the electrode sheet.

When the electrode is sucked on the low-pressure vacuum-suction gripper, the third stage begins and the acceleration of the suction roll starts. At this stage, the electrode sheet is pulled down from the electrode stack through the suction roll, slides over it and hits the slit of the conveyer belt with the lead edge.

The fourth stage begins when the lead edge of the electrode sheet handling is transferred from the suction roll to the conveyor belts. From this point, the sheet is jammed between the belts and will be transferred to the end of the machine.

In summary, tensile forces, bending forces and, probably, shearing forces occur during the four phases of the separation process (Table 1). All these specific loads may lead to different external damages (coat chipping, cracks, elastic and plastic deformations, delamination), which could influence the electrochemical performance of the cell.

Table 1. Results of the process analysis of the separation module from the first step of the method.

	Overview of the Loads on Electrode per Stage
1. Stage	No loads.
2. Stage	Bending loads occur through the upward movement of the electrode. Tensile force on the suction area through the suction roll. The impact of the electrode on the suction inlet of the vacuum roll can lead to local chipping of the coating and to deformations.
3. Stage	Tensile force in the conveying direction occurs due to the acceleration of the vacuum roll and the mass inertia of the electrode. Impact loading occurs when the leading edge of the electrode hits the belt drive but does not optimally hit the slit. This can lead to chipping at the leading edge of the electrode.
4. Stage	Deformations can lead to shear stresses, which may occur due to a badly synchronized movement of the electrode to the conveyor belt. In case of large deformations, delamination and collisions with the machinery occur.

2. Step—Identification of material models | In the second step of the method, the identified stresses on the handled electrode during the separation process are analyzed and assigned to suitable material models, which have to be compared with each other in terms of their quality. The electrode being handled and stressed consists of a substrate foil made of aluminum or copper and a specific coating, depending on the type of electrode (anode or cathode). Since the aluminum or copper foil is a rolled intermediate product, whether an anisotropy factor due to the rolling direction influences the otherwise isotropic material behavior should be checked. The coating consists of various particles in different sizes, which are mixed with a binder and applied to the carrier film, and which have a homogeneous behavior. However, since the coating is still rolled (calendared), anisotropic properties can also arise.

Since the electrode is a layered composite with two potentially anisotropic materials, it was considered that, in addition to the otherwise simple isotropic linear material model, non-linear and anisotropic material models should also be included in the investigation.

3. Step—Material characterization | For the identified material models, the necessary characteristics are carried out in step three, which subsequently allow the material models to be built. In order to represent the stresses correctly, deformations due to the load must be represented as accurately as possible. The direction and stress-dependent strain, which can be determined with the help of material tests, is used as an equivalent for the deformation in the material model. Depending on the material model, different material tests have to be realized, which can start with uniaxial tensile and compression tests, biaxial tensile tests, and end with pure shear tests. Within the framework of the investigations, it was sufficient to carry out uniaxial tensile tests with the electrodes.

The potential anisotropic behavior was checked by taking and comparing samples in the rolling direction (MD) and orthogonal to the rolling direction (TD) of the electrode. Comparing the results of the tensile tests with each other, there is no significant anisotropic behavior for the electrodes used for this investigation. However, this does not mean that the statement is generally valid.

4. Step—Create and validate material models | In step four, the collected data from the material characterization were utilized to design the identified material models. After the material cards are created, the tensile test is modeled and simulated. In the simulation, the material models are assigned to the tensile specimens and the uniaxial tensile test can be simulated. After all material models have been used, the resulting stress–strain curves can be overlaid with the real tensile test data (Figure 4). It is evident that the elasto-plastic isotropic material model predicts the real material behavior of the anode very well. This procedure was also used for the cathode, and it turns out that the elasto-plastic isotropic material model is best suited to simulate the material behavior of the cathode.

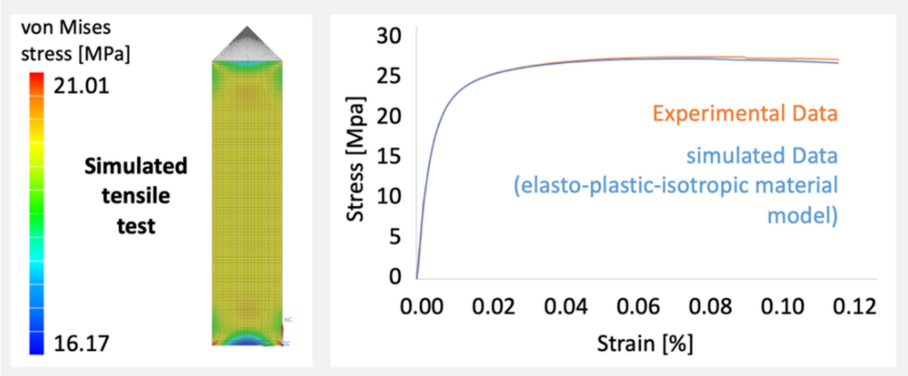

Figure 4. Exemplary validation of the anode material model.

Due to the good results of characterization and material modelling, it is now possible to continuously represent more complex loading cases, since the material behavior can be represented very well. Nevertheless, it is important to note that the entire handling process should take place in the elastic range only. Otherwise, irreversible damage to the electrode will occur, which affects the electrochemical performance of the cell.

5. Step—Model and simulate sub-process | After all critical sub-process steps of the separation module have been identified in step one and the corresponding material models have been created in step four, each sub-process step is now modelled and simulated in step five. By creating the model, it should be ensured that a computationally efficient model is created to ensure that the relevant parameters can be specifically designed in an optimization loop afterward. Figure 5 illustrates how the initially complex CAD model of the assembly was idealized, as far as possible, to the most essential simulation-relevant components. Depending which process is depicted, it should be considered which elements have an influence and to what level of detail they need to be represented. In the shown use case of the separation module, all contact areas of the handled electrode have been implemented accordingly. Since there may also be flexible elements such as belts, etc., it should be considered to what degree of detail these characteristics are taken into account and what influence they have on the target values sought.

With the aid of the idealized assembly from Figure 5, all four sub-process steps could be represented with the use of a coupled CFD-FEM simulation. By coupling the sub-process steps, it is possible to consider dynamically conditioned load variables and to physically represent the real case of separation in the simulation as accurately as possible. Through the coupling, deformations and stresses of the electrode from the initial position in the magazine to the ejection or the transfer to the paddle wheel are included in the simulation. As an example, Figure 6 shows the stress on an electrode as it passes through the simulated coupled sub-process steps of the separation module.

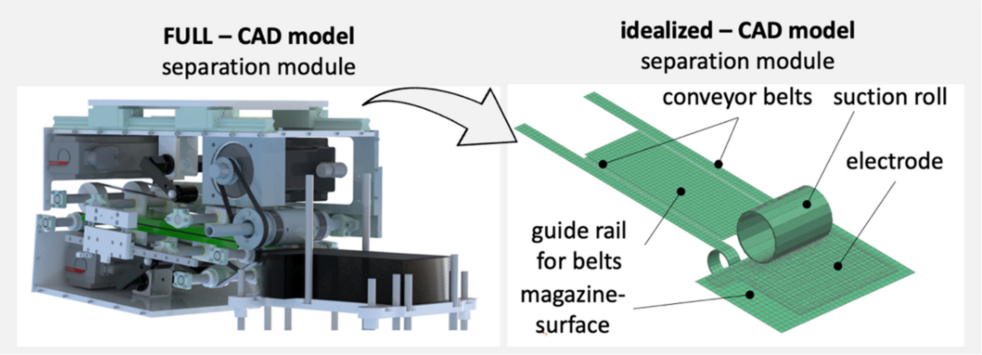

Figure 5. Idealized model of the separation module representing the essential components that are necessary for the simulation of the subprocess.

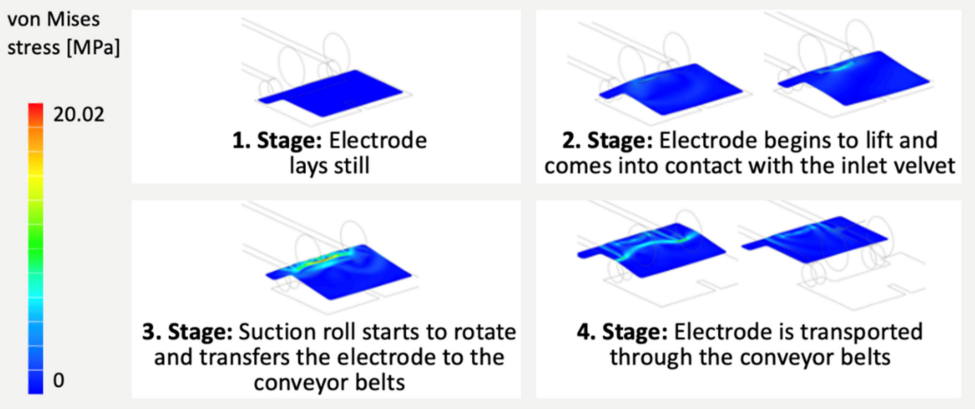

Figure 6. Stresses on the electrode are shown as a sequence for the separation module.

Starting from the rest position of the electrode in the magazine (Figure 6—top-left), it can be seen how the electrode has lifted and the initial contact between the suction roll and the electrode has been produced (Figure 6—top-right). After initial contact with the suction slot of the vacuum roll, the vacuum inside the roll increases rapidly and ensures that the electrode adheres firmly across all suction holes of the rotating low-pressure vacuum-suction gripper. The increased stress values can be recognized by the changed color spectrum (Figure 6—top-right), which is generated by the yielding adjustments of the electrode foil. Figure 7 shows this stress condition in detail. It is obvious that spacing, diameter and position of the suction insert as well as the number of rows have a significant influence on the contact pressure of the electrode, which need to be investigated.

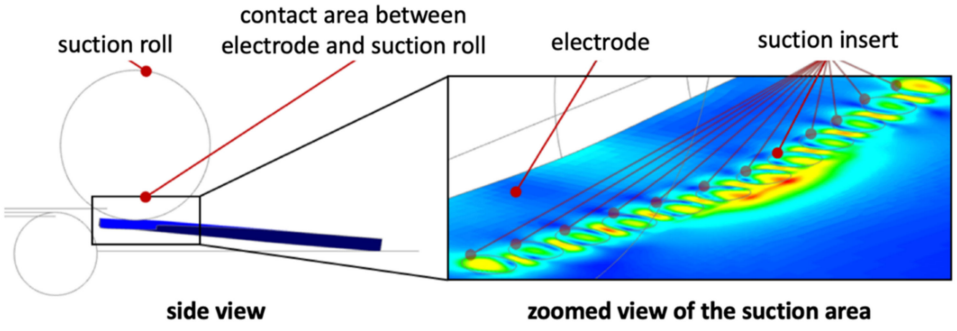

Figure 7. Detailed view on the optimized contact area from the air inlet of the suction roll and the electrode.

In the following, it is shown how the electrode is transferred to the conveyor belts (Figure 6—bottom-left) and a shear stress is induced. This shear stress occurs as the electrode is transported away from the conveyor belts and is held by the suction roll at the same time. This load represents the biggest stress on the electrode and can only be identified by the help of the simulation. This shows that a process simulation is not only used to validate the design of the process assembly but should also be used to analyze the stress on the product. The results of this simulation were therefore decisive for the constructive design of the assembly, to ensure a low-shear stress transfer to the electrode. After the electrode has been released from the vacuum roller (Figure 6—bottom-center), it is shown how the stress is relieved and continues to decrease as the electrode is transported away (Figure 6—bottom-right).

6. Step—Derive process limits through optimization | In step five it was shown that a coupling of the partial process steps of the separation module could be successfully implemented. The high resolution of the models allows a purposeful simulative design of the elements that are used to handle the electrode.

Through the coupled simulation, it is therefore possible to modify the microstructure of the suction insert of the vacuum roll in terms of shape, number and arrangement and to optimize it regarding the material limits and the associated process limits (Figure 7). It is naturally also possible to optimize further design elements of the separation or to identify suitable process parameters by optimizing the parameters of the system with regard to the process limits.

Summary of the case study | The approach could be applied to the separation module of the stacking process with low effort. The motivation was to optimize the existing prototype regarding its throughput by specifically redesigning individual module parameters. With the help of a model of the system, it was possible to compare various configurations without significant effort. The focus of the approach was always on the object to be handled, which defines the boundary conditions for the process step. By applying the method, a model of the separation module has been created, which can validate new formats in advance without great effort. The process model also makes it possible to test and optimize new characterized materials parallel to the operation of the plant. Consequently, shorter set-up times result in case of a future material change.

3.1.5. HoLiB—Paddle Wheel

1. Step—Process analysis | In robot-based pick-and-place processes, pneumatic grippers are established for handling the delicate electrodes. The area vacuum grippers create a gripping force through multiple small suction holes. This principle reduces pressure peaks and leads to low mechanical loads on the gripping surface [39]. In contrast, the paddle wheel process applies mechanical handling devices, such as end stops and skids, to position and orientate the electrodes. The mechanical handling devices induce mechanical loads on the material, which differ from the ones known from robot-based handling.

A preceding analysis shows that the main process forces are frictional forces and impact forces and identifies four main process phases, as shown in Figure 8. In the first process phase, a conveyor belt inserts the electrode into the paddle wheel with a target velocity of 1500 mm/s^{-1}. During this phase, the electrode performs an uncontrolled free movement before it collides with the paddle. The collision leads to an abrupt deceleration of the electrode. This is the second phase of the process. The most important contact area during this phase is the edge of the electrode. The third process phase is the transportation phase. During this phase, the surface area of the electrode abuts one of the paddles. The mechanical loads during this phase are low. However, when the electrode reaches the top of the wheel, it turns over from one paddle to the next one. This causes a short load on the electrode surface. The fourth phase is the ejection phase. During this phase, the electrode collides with an end stop and slips out of the paddle wheel onto a tray. The end stop is necessary to ensure a constant ejection position. Without the end stop, the stick–slip effect and electrostatic adhesion influence the ejection position strongly and inhibit a robust

ejection process. Similar to phase two, the majorly stressed area during this phase is the edge of electrode, as it collides with the end stop at a high velocity.

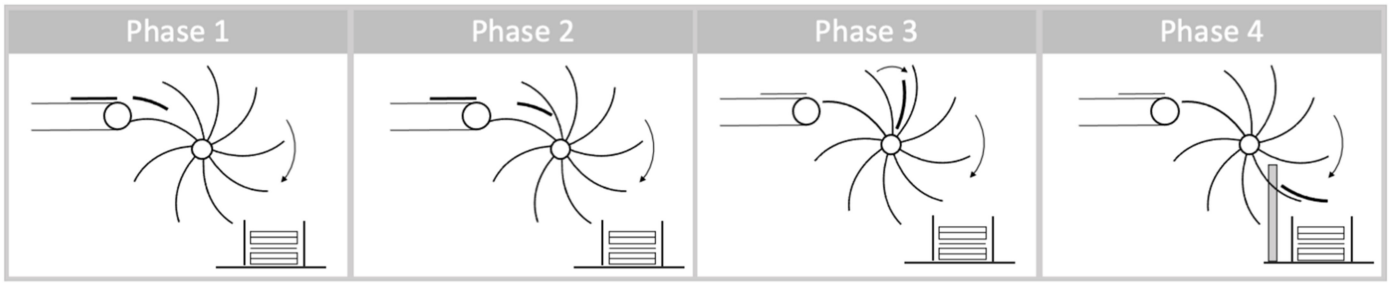

Figure 8. Process phases of the handling process in the paddle wheel.

It is essential to identify the influence of machine parameters in order to mitigate the mechanical loads during the process. A process simulation supports the identification of suitable process limits and parameter settings of this novel process. It is also necessary to identify the maximum acceptable forces to avoid critical loads and material failure.

2. Step—Identification of material models | An efficient method of describing the process is a dynamic multibody simulation (MBD). In this study, MSC ADAMS is chosen as the software tool for the MBD. An MBD indicates the forces occurring between the electrode and the wheel and describes the motion of the electrode during the handling process. The thin electrode is modelled as a flexible foil, as proposed in [40,41]. The wheel and the paddles are thick compared to the electrode and, therefore, they are described as rigid bodies. A modal neutral file (mnf) generated in a modal analysis is used to model the flexible electrode. The results of the modal analysis depend on the mesh and the material model. For a realistic flexible multi-body simulation, it is necessary to validate the modal analysis. A perfect validation of a modal analysis requires highly complex measuring tools. Therefore, it is favorable to focus on the relevant process characteristics rather than a complete model of the flexible electrode. The relevant characteristics for edge contacts is the coefficient of restitution. This indicates whether the electrode remains on the paddle or flips out of the wheel during the insertion process. Additionally, by defining the coefficient of restitution, it is possible to identify plastic deformation during the contact. It is necessary to inhibit plastic deformation to avoid damaged electrodes leading to a poor electrochemical performance of the cell.

3. Step—Material characterization | To characterize the effect of edge contacts, controlled and repeatable edge collisions are performed in special test rig. The test rig works like a hatchet where the electrode drops onto an impact surface at the base of the test rig. It is possible to vary the dropping height of electrode, collision angle, size and material of impact surface. To characterize the bouncing effect of the electrode, a camera was installed at the bottom of the test rig. Figure 9 shows the elements of the test rig.

The first analysis is the characterization of the bouncing effect of the electrode. For this analysis, a fixed dropping height of 150 mm and a collision angle of 0° are set. The material of the electrode (anode) is 94% graphite, 2% CMC, 3% SBR and 1% C65 on a 10 µm copper substrate with the size of 50 × 70 mm^2. The mass load of this anode is 9.2 mg/cm^2. During the drop of the electrode, a video analysis records the edge collision. The video sequence shows the bouncing height of the electrode and, thereby, enables calculation of the coefficient of restitution. Figure 9 shows a shot from the video sequence. Each drop test is performed five times with the same electrode.

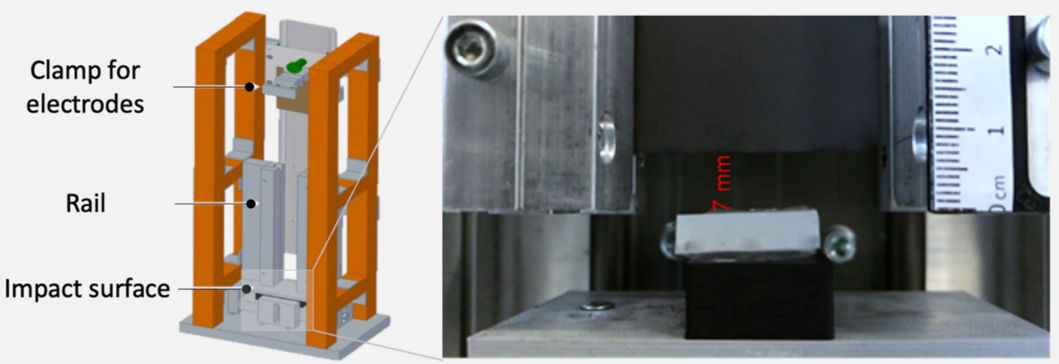

Figure 9. CAD Model of edge collision test rig (**left**) and a close-up of a bouncing electrode (**right**).

The analysis shows a high influence of the material of the impact surface on the coefficient of restitution. For soft materials, such as plastics with a thin layer of silicone 13 ShA, the coefficient of restitution of the tested anode is higher than for hard materials, such as aluminum. Table 2 shows the results of the measurements.

Table 2. Measurements from the edge collision test rig.

Material of Impact Surface	Coefficient of Restitution
Aluminum	0.04
PLA + Silicone 45 ShA	0.15
PLA + Silicone 13 ShA	0.22

The experiments in the test rig for the edge collision also show characteristic damages of the electrodes. An optical investigation of the deformations under a light microscope shows three main types of damages due to edge collision: cracks and ablation of the active material, as well as deformation. Figure 10 shows the different types of damages for a cathode edge as recorded with a KEYENCE VHX-2000 light microscope. The cathode material used in the experiments is 95.5% NMC-622, 3% additives and 1.5% PVDF on a 15 µm aluminum substrate. The mass loading of this material is 17.3 mg/cm^2 and the size of the electrode is 65 × 45 mm^2.

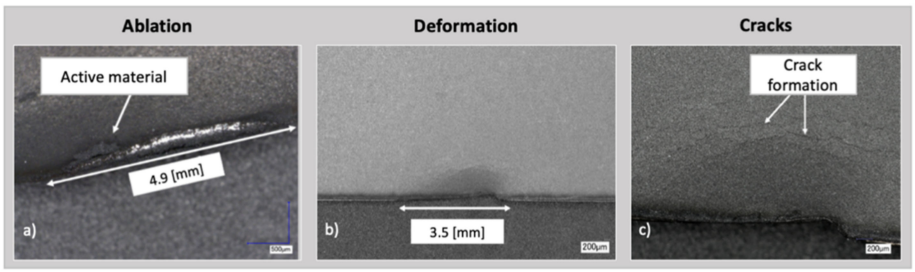

Figure 10. Visualized types of damage caused by the edge collision on a cathode edge.

In order to describe the contact between the electrode and the wheel in a proper manner, it is necessary to determine the friction coefficient. Table 3 shows the friction coefficient for different materials. In general, the friction coefficient for the cathode is higher due to the good anti-friction properties of the graphite anode.

The simulation focusses on the combination POM/Anode and the friction coefficients being set accordingly. Nevertheless, it is possible to simulate other material combinations with low effort.

Table 3. Measurements from the edge collision test rig.

Tribological System	Static Friction Coefficient	Dynamic Friction Coefficient
Aluminum/Anode	0.25	0.19
Aluminum/Cathode	0.3	0.26
Silicone 45 ShA/Anode	0.87	0.75
Silicone 45 ShA/Cathode	0.99	0.8
POM/Anode	0.24	0.17
POM/Cathode	0.29	0.23

4. Step—Create and validate material models | To simulate the bouncing effect, an MBD is set up that simulates the collision of the electrode with a static wall. Afterwards, a comparison of the simulation results and the measured bouncing height in the test rig takes place to validate the simulation parameters.

The contact force between two bodies depends on the following simulation parameters: the stiffness coefficient k, the force exponent e, the damping coefficient c_{max} and the penetration depth d. The parameters mentioned are variables of the impact function. The impact function describes the contact between two bodies in a multibody simulation as [42]:

$$F_N^i = \begin{cases} kx^e - c_{max}\dot{x}\ Step(x,0,0,d,1) & if\ x > 0 \\ 0 & if\ x = 0 \end{cases} \quad (1)$$

The stiffness coefficient k relates to the elastic modulus and the geometry of the simulated bodies [43]. The solution for k can be determined by solving the differential Equation (1). The integrated solver of MSC ADAMS provides a solution for the equation with $k = 1.65e + 6$. Accordingly, c_{max} is set $1.65e + 2$ or 0.01% of k [42,43]. References [42,44] introduce a penetration depth of 0.1 mm [44] and validate $e = 2.2$ as a standard value for hard materials. With this set of parameters, the validation of the bouncing effect is conducted. The motion of the electrode is tracked with the help of post-processing tools. The bouncing height in the simulation is 8 mm. The bouncing height in the test rig according to the video analysis varies from 0.3 mm for aluminum up to 2.9 mm and 7.3 mm for PLA + silicone 45 ShA and PLA + silicone 13 ShA. The value for PLA + silicone 13 ShA is close to the measurements from the simulation.

5. Step—Model and simulate sub-process | As described in Section 3.1.4, it is reasonable to replace the complex CAD model with a simplified model and focus on the main components of the process. In the simulation model, the wheel is modeled as one single body (Figure 11—right) replacing an assembly of various parts in the CAD model, such as paddles, mountings and a hub (Figure 11—left).

Figure 11. CAD model (**left**) and simplified simulation model (**right**).

Another simplification in the simulation is the contact between the electrode and the conveyor belt. This contact is set as a frictionless contact. Section 3.1.4 describes the

simulation of the contact forces between the electrode and the conveyor belt in detail, so it is not necessary to analyze them in this context. Instead, the analysis focuses on the contact forces between the electrode and the wheel. The static and the dynamic friction coefficients are set as described in step two.

Now, the simulation is used to investigate the bouncing effect of the electrode during the insertion process. After the collision with the paddle, one would expect a sudden movement of the electrode in reverse direction, as the analysis of the bouncing effect in step four demonstrates. However, no such movement occurs in the simulation of the paddle wheel process. There are two main reasons for this observation: First, in contrast to the bouncing simulation and the test rig, where the impact surface is fix, the paddles of the rotating wheel are not fixed. They move in the same direction as the electrode. Therefore, the collision leads to a decrease in the electrode velocity in horizontal direction, but the electrode does not stop. Second, the paddle has a curved shape. Instead of bouncing, the edge of the electrode moves along the curvature of the paddle.

The simulation results show a contact force of 718 N for the simulation of the test rig. In the wheel, the contact forces with the paddle depend on the rotational velocity. For the target rotational velocity of 37.5 rpm, the simulation shows a contact force between the electrode and the paddle of 341 N. Given that the simulated forces of the test rig are twice as high as the simulated forces in the wheel, the damages as described in step four are expected to be less severe in the paddle wheel than in the test rig.

6. Step—Derive process limits | The simulation has shown that a successful insertion of the electrode is possible. The shape of the paddles and the rotational velocity of the wheel support a successful insertion process, as they reduce the bouncing effect of the electrode. The electrode remains in the wheel and there is no bouncing effect.

The experiments in the test rig show damages of the electrode. The damages in the paddle wheel are expected to be less profound, as the simulation shows significantly higher forces for the test rig. However, the damages require further investigation. To estimate the effect of the edge defects on the electrochemical performance, damaged electrodes are assembled to pouch cells with one anode, one cathode and a separator and a capacity measurement is performed. In this setup, the edges of the anode are 5 mm longer than the edges of the cathode to make sure that the anode completely covers the cathode. Consequently, edge defects of cathodes have a higher impact on the electrochemical performance of the cell, as the edges of anodes may not participate in the electrochemical reaction. Therefore, the cathodes undergo edge collisions in the test rig for this series of experiments. There are four different batches of cells. The *reference* cells have no edge collision. For the batches at 0° and 10°, cathodes were dropped onto the impact surface at a collision angle of 0° and 10°, respectively. For the batch *double*, the electrode faces two edge collisions before the cell assembly. Each batch comprises three cells. Each cell undergoes six charging and discharging cycles with 0.2 °C. The dropping height in the experiments is 200 mm to reinforce the effects of the edge collision.

Figure 12 shows the charging and discharging capacity of the test cells. The edge collision leads to higher capacities compared to reference cells. The edge collision leads to deformation and folding of the electrode. A small section of the electrode surface folds over at the edge of the electrode. This might lead to shorter diffusion paths of the ions on the backside of the electrode. Consequently, a small section of the backside of the electrode may take part in the electrochemical reaction, leading to a higher capacity. The backside taking part in the electrochemical reaction can lead to a disadvantageous balancing within the cell. Therefore, further investigations should include the long-term performance of these cells. Another effect is a higher deviation between the values. This is especially the case for the batch *double*. As the sample size of the experiments is small, further investigations with a larger sample size should be conducted to prove the results.

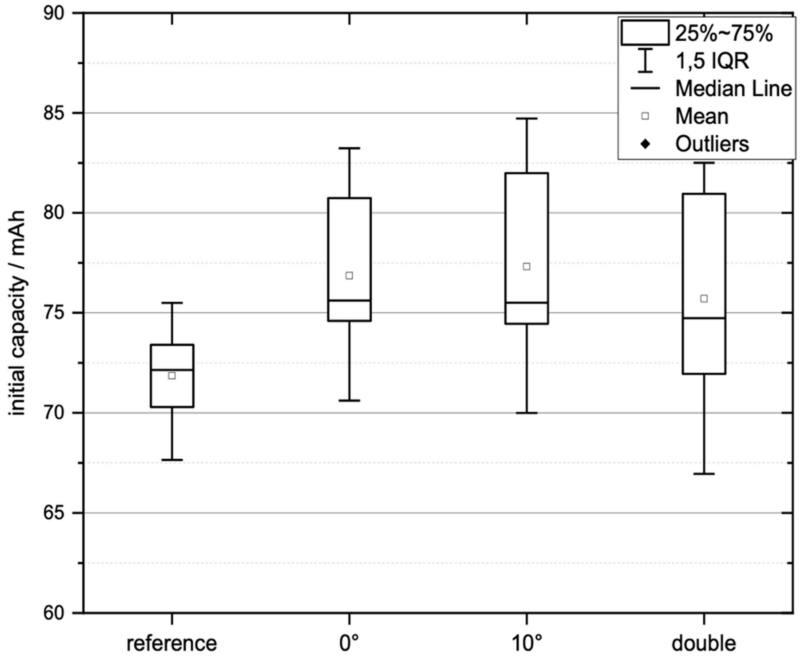

Figure 12. Discharge capacity of edge collision cells and reference cells.

Additionally, further investigations need to verify whether the effects of edge collision are still dominant for large multilayer cells. The investigated cells are small and consist of one layer. The edges are long in comparison to the size of the electrode sheets. Nevertheless, it is crucial to reduce the induced forces during edge collision to avoid defects. The simulation supports comparison and optimization of process parameters such as rotational velocity and paddle curvature.

Summary of the case study | The handling of electrodes with the paddle wheel leads to contact forces between the electrodes and the paddles. These forces can lead to undesirable effects. The electrodes bounce back and flip out of the wheel. Moreover, a deformation of the electrode can occur with an impact on the electrochemical performance of the cell. A simulation model, based on multibody dynamics, can predict the electrode motion and the occurring contact forces during the handling process. The simulation can indicate the effects of different process parameters, such as the rotational velocity or the shape of the paddles. Based on this information, the choice of a favourable set of parameters for the process is possible. However, the impact of the edge collision on the electrochemical performance is partially uncertain and there is a need for further experimental investigation.

3.2. KontiBat—Productivity Increased Z-Folding Ies Using Continuous Processes

3.2.1. General Process Description

The KontiBat project aims to increase the throughput in ESC assembly by converting sequential process steps to continuous. The continuous approach eliminates the throughput-limiting pick-and-place operations and enables lower cycle times. The material provision is discrete for electrodes and web-based for the separator. Figure 13 shows the process architecture of the continuous ESC assembly. The magazine change unit provides the electrodes for the subsequent separation unit. These electrodes are accelerated from the stacked state and fed to the electrode joining unit. In the separator feeding unit, the web-based separator is unwound. The separator is fed through an edge guiding and a web tension control system at a constant speed into the electrode joining unit to be joined alternately with anodes and cathodes. Unlike other research activities, the joining process is not performed by lamination, but by comparatively low-cost and high-throughput gluing process. After gluing, an endless and unfolded ESC is formed, which is then fed into the

z-folding. The z-folded ESC is stacked and secured on a stacking table by the cell handling unit. Functional ESC with a predefined number of layers is fed out of the system.

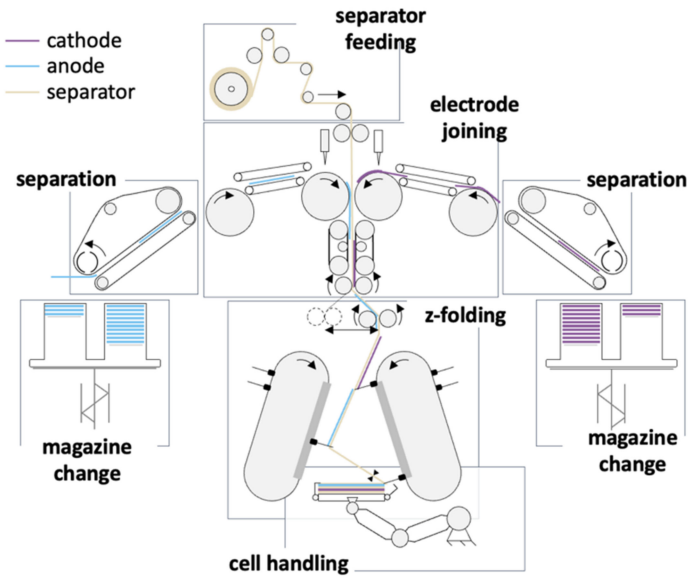

Figure 13. Architecture of the ESC assembly process in the research project KontiBat [8].

3.2.2. Reasons for Simulation-Based Process Modelling

The gluing of electrodes with a separator represents a process-specific special operation. While the electrodes are still being fed, an adhesive is applied to one side of the electrode while maintaining a constant feed rate [45]. The challenging material properties of the web-based separator combined with the targeted feeding speed for high-throughput ESC assembly result in strong interactions between process and machine parameters and product quality. The behavior of the separator, which is fed into the joining unit with defined web tension, and the spot gluing with the electrodes is unknown and has to be investigated due to the novelty of the joining concept. It is assumed that due to the structural limitation caused by the glue dots, wrinkling of the separator may occur.

The quality feature of the z-folding in ESC assembly is the alignment of the longitudinal edges, whereby the highest possible degree of coverage of the electrode sheets in the stack is achieved. The alignment of the longitudinal edges can only be achieved if the separator material is folded orthogonally to the machine (longitudinal) direction. To prevent piling up of the stack at the folded edges, the folds must be sharp-edged. The z-folding as the value-adding handling and joining function highly influences the surface coverage of the electrodes within the stack and, thus, the overall ESC quality. The interdependencies between the web tension, the gripper geometry, the accuracy of the transport system and the ESC are not known, and must therefore be investigated. Furthermore, the web tension must be limited in such a way that the material is not damaged the disturbing influence on the accuracy can be controlled by the drive system and, at the same time, quality-assured z-folding will be possible.

As described in Section 3.1.2, it is appropriate to use a simulation of the processes to gain specific knowledge about loading effects during z-folding and to use this knowledge in the design, parameterization and control. Accordingly, a simulation of the z-folding process can be used to specifically analyze the deformations of the glued ESC. The aim is to find a material and format specific parameter set where no damage of the ESC occurs.

3.2.3. Disadvantages of an Empirical Approach

The gluing of the separator and electrodes is a novelty in ESC assembly. No previous knowledge is available to design the process and machine. A purely empirical approach would be associated with a high level of effort and correspondingly high costs. Additionally,

the design of process and machine parameters for gluing, e.g., the type and number of gluing spots are unknown. These parameters are further dependent on the separator and electrode as well as on the format. With a model-based development approach, material and format specific process and machine parameters can be examined and interdependencies can be identified and used for other material and/or formats.

3.2.4. KontiBat–Z-Folding Process

1. Step–Process analysis/loads on intermediate products | The material flow during high-throughput ESC stacking is first investigated analytically. A key unique feature of the high-throughput ESC stacking is the feeding of the separator material and electrode sheets at a constant velocity, and the subsequent z-folding. Based on the derived kinematic relationship of z-folding by Glodde [46,47], the z-folding kinematic is considered idealized as a two-dimensional system, since the folding motions occur in one plane. The path-time diagram of one gripping system is shown in Figure 14 as an example for the reference format with 304 × 129 mm (length × width), a separator feeding speed of 500 mm/s and a circulation length of the transport system of 2500 mm. Starting at the point of gripping the endless and unfolded ESC, the counting of the distance traveled starts. The transport system is divided into the sections of folding, return, synchronization and gripping. In the first section, the gripping system decelerates from the original nominal machine speed and comes to a short stop in the folding plane at 650 mm. At the end of this section, the folding point must be moved along a circular arc to maintain the web tension in the separator. After leaving the folding section, the gripper system resets in the following section, which contains acceleration and deceleration phases. The following third section is used for synchronization on the fed ESC in order to be able to again grip the material at the defined time and position in the fourth section.

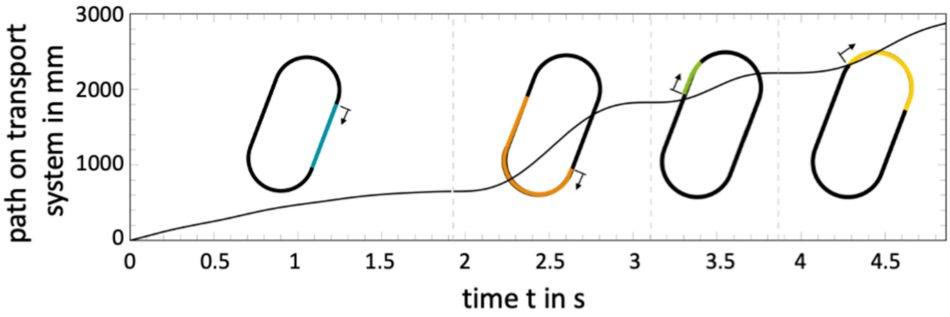

Figure 14. Curve of distance traveled by the gripper on the transport system using the example of the reference format with 304 × 129 mm; one-sided representation of the z-folding unit [8].

The analytical consideration of the movements shows that that cycle times for gripping and z-folding the unfolded ESC cannot be linearly scaled to different cell formats. The cycle times for the opening and closing movements of the gripping systems for different cell formats can be derived from the analytical kinematic model. These times are necessary for later use in the dynamic process simulation.

A parallel gripper with a normally open working principle was selected through earlier works [37]. For the realization of the gripper closing movement, different constructive designs are possible, such as a one-sided gripping jaw or two gripping jaws, which move towards each other. For each of these designs, the engagement depths must be identified. The engagement depth is given relative to the width of the separator. Considering large separator widths, the one-sided gripping jaw movement could pose a time challenge for the drive and the kinematic structure of the gripping system. When using two gripping jaws moving towards each other, the distance per side is halved, but at the same time, there is no knowledge of the minimum required engagement depth so that the separator belt can buckle in the middle.

Aside from the cycle times, the reaction forces are also decisive for dimensioning the z-folding process. Analogous to the motion profile, the reaction force acting on the gripper system due to the web tension is not linear. The resulting reaction force on the gripper system increases in the folding area from zero to approximately twice the web tension force, and reaches its maximum value in the folding point at 650 mm. This force curve will be later used in the dynamic process simulation.

At the end of the folding process, the separator material, which remains under web tension, is clamped on the stacking table, while the movement of the gripping system causes the separator to wrap around the gripping jaws. The separator is under a combined load with tension, compression, bending and shear, whereby the electrodes are only loaded with tension and compression.

2. Step–Identification of material models | In handling operations for single sheet stacking, electrodes and separators must not suffer any plastic deformation, while the goal of z-folding in ESC stacking is plastic deformation of the separator at the folding point. As the electrodes are only loaded with tension and compression during z-folding, the isotropic linear-elastic material model presented in Section 3.1.4 is used here, as well.

Depending on the type and manufacturing method of separators, the separators may have a directional dependency. Dry membranes and composite separators are known to behave anisotropically, whereas wet membranes do not exhibit any clear anisotropy. Since the anisotropy of the material plays a significant role in a multiaxial loading situation, this property must be considered in the material model development and selection. In order to simulate the forming process by z-folding, the material model for separators must represent elastic as well as plasticity effects. The following step describes the experimental characterization of the separator material.

3. Step—Material characterization | Uniaxial tensile tests are performed to identify the material behavior and derive constants of the stiffness matrices (Young's modulus and Poisson's ratio) for separators. In the tensile test, standardized specimens are stretched until a predetermined strain is reached, or until the material fails completely in the form of a fracture. The tensile tests on separators in this work were carried out in accordance with the DIN EN ISO 527-1 standard. A rectangular strip shape is selected to determine the material properties. This simple shape allows reproducible manual specimen preparation by cutting with a scalpel. The length of the strip is 150 mm and has a width of 20 mm. The initial spacing between the grips in the tensile test is 106 mm.

To determine the direction-dependent material properties, cutouts of the specimens are made in MD, TD and, additionally, in the diagonal directions (DD+ and DD−) for the separator (Figure 15). A mechanical investigation in thickness direction is not possible due to the low material thickness [48]. In order to determine the visco-elastic behavior of the separator, tensile tests are carried out at different test speeds. Since ESC assembly takes place in a conditioned atmosphere, no temperature variations are expected, and the temperature-dependent influence is not investigated here.

In Figure 16, the exemplary stress–strain diagram of a ceramic separator shows a strongly anisotropic behavior. This anisotropic behavior can be reduced to orthotropy by considering the microscopic structure and the manufacturing method. The separator has the highest stiffness in MD, followed equally by DD+, DD− and TD. The diagonal material directions DD+ and DD− show only small differences. The stress–strain behavior in the elastic region shows an approximately linear increase, which takes a linear course after reaching the equivalent yield strength. With respect to the strain rate dependence, a weak expression is shown in the elastic range, whereas a clear dependence can be seen in the plastic range, especially in MD.

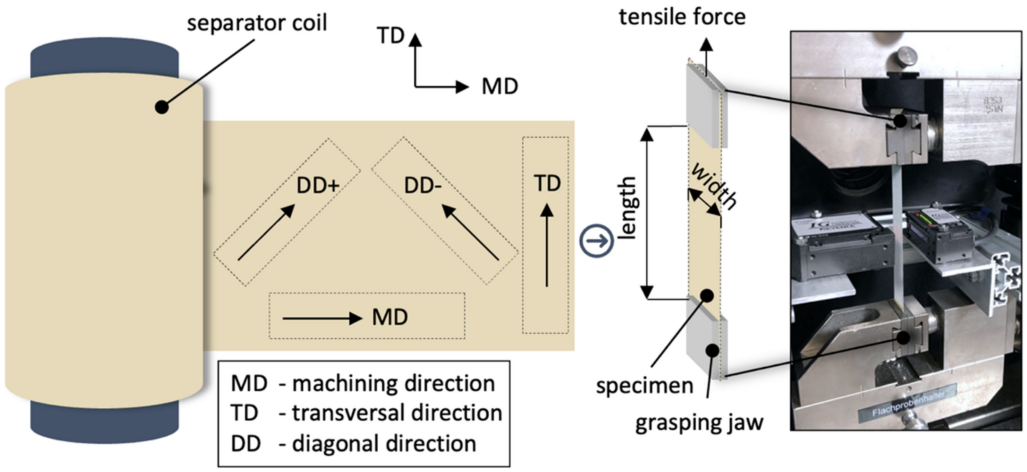

Figure 15. Shape, dimensions and cutout positions of the specimens; DD directions are rotated by 45° or 135° with respect to MD [8].

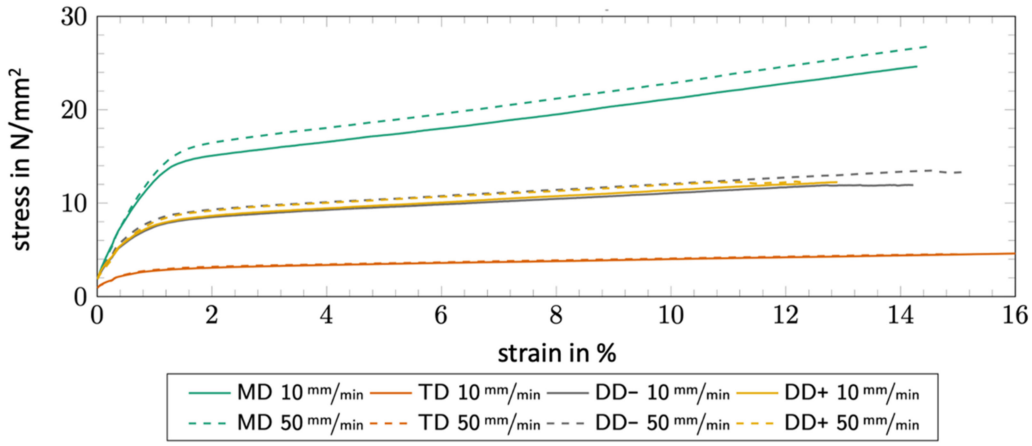

Figure 16. Stress–strain diagram of ceramic separator [8].

4. Step—Create and validate material models | After the material characterization of the separator and the initial evaluation of the material behavior, the identified material characteristics are used to create the material models.

The tensile tests have shown that separators exhibit an orthotropic behavior. Moreover, for the simulation-based investigation of process limits for ESC stacking, the plastic range as well as the elastic range has to be considered. Nine independent material parameters are required to describe the elastic behavior. For the Young's modulus E1 and E2, the values for MD and TD are used, respectively. The Young's modulus in the thickness direction cannot be determined due to the small thickness of the separator, so that the Young's modulus in the TD direction is used as a substitute [48]. Furthermore, the averaged DD value is assumed as shear modulus [48].

The orthotropic–plastic behavior is described with the aid of Hill yield criterion [49]. For this purpose, scalar parameters are introduced that describe the state of orthotropic hardening. These parameters are calculated using the determined stress–strain curves.

The creation of the material model includes the step of validation, in which the simulated material behavior is compared with the experimentally determined values. The results of the linear–elastic orthotropic material model show good agreement with the experimentally determined course, up to a strain of approximately 1% (Figure 17). The plastic region is reproduced with high agreement. In TD, the elasto-plastic orthotropic material model provides good agreement, although the stresses for strains greater than 1.5% are slightly higher in comparison. It is evident that the elasto-plastic orthotropic

material model predicts the material behavior of the separator over the entire strain range in MD and TD very well. This material model is selected for the following investigations.

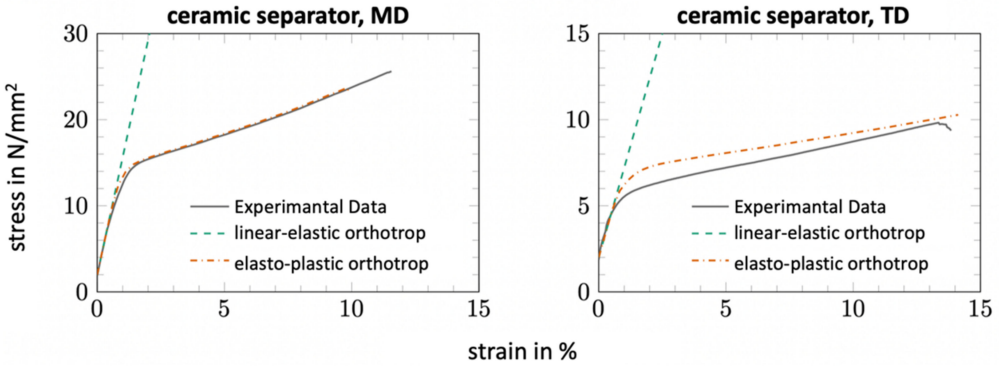

Figure 17. Stress–strain curves of different material models for ceramic separator in MD and TD [8].

5. Step—Model and simulate sub-process | The simulation-based investigation of material behavior for different process and machine parameters as well as materials and formats require an idealized model of the real z-folding process. The following idealization is used for modeling (Figure 18):

- The idealized model considers the process of folding a strip of separator with a total length equal to twice the battery cell length (2 × 304 mm).
- The separator is clamped at one end with web tension acting at the other end.
- The clamping jaws of the gripper are positioned at the region of the separator to be folded (folding line).
- Different engagement depths are controlled by the length of the clamping jaws.
- One anode and cathode are arranged alternately on each side of the separator.
- The adhesive connection is modeled simplified as a rigid connection between separator and electrode. A total of four glue points are provided for each electrode.

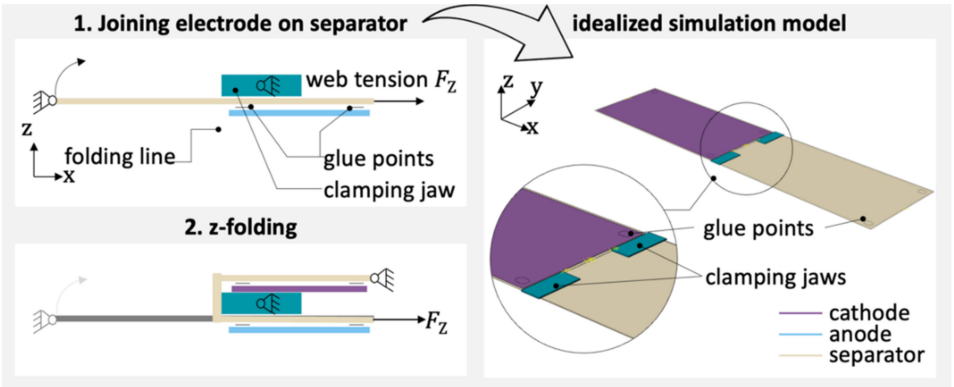

Figure 18. Idealization of z-folding process for simulation (**left**) and simulation model (**right**) [8].

To simulate the folding motion, the left edge of the separator is rotated around the y-axis, while the acting web tension force at the right edge is kept constant. Since the bending deformation of the separator at the fold line considered here does not represent a static load case and is time-dependent, a dynamic–explicit simulation step is performed. The total duration of the folding movement corresponds to the format-dependent duration of the z-folding process and is taken from analytical calculations.

In order to evaluate the influence of process and machine parameters with the aid of simulation, quantifiable quality characteristics of the z-folding process must be selected. For the structural mechanics problem of separator wrinkling, strains and stresses are defined as quality characteristics to be investigated.

The Figure 19 shows the normal stresses in the x- and y-directions for a two-sided engagement of clamping jaws and web tension with 3 N and 4 N at the end of the folding motion. For the visualization areas with a higher stress than the direction-dependent equivalent, yield strengths are gray colored.

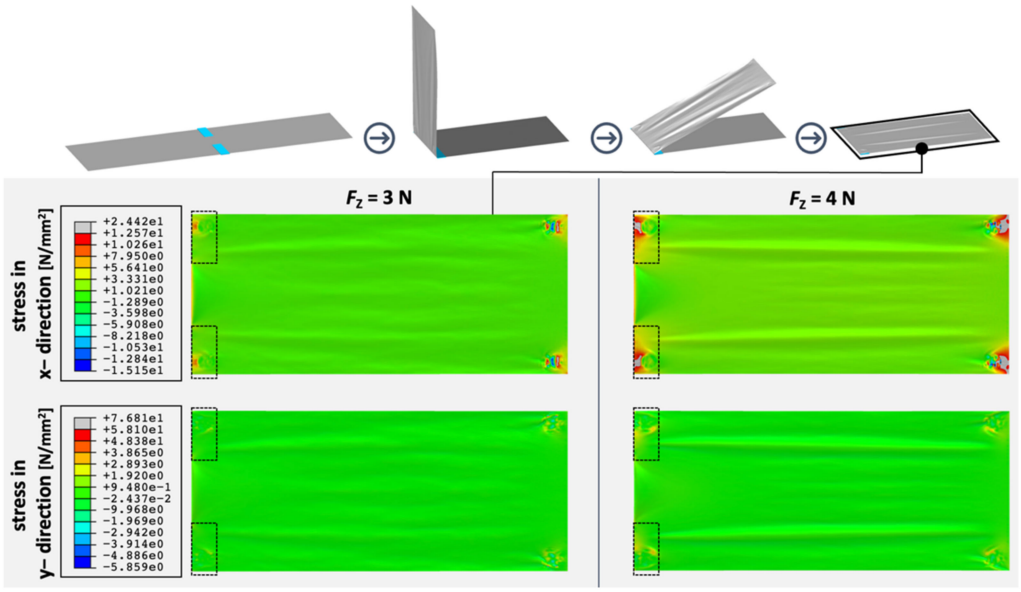

Figure 19. Normal stresses in x- and y-directions at the end of the folding motion for the ceramic separator and different web tension [8].

When observing the normal stresses in the x-direction, high stresses always occur in the areas between the gluing spots and the clamped edges of the separator. For the case of web tension of 4 N, a small plastic deformation of the ceramic separator between the gluing spots and the clamping edge on the right is predicted by the simulation, while no plastic deformation is expected when the web tension is reduced to 3 N. When considering the normal stress in the y-direction, the equivalent yield strength is not exceeded, even with a web tension of 4 N.

Further simulation-based investigations have shown that greater engagement depths of grasping jaws and lower web tension lead to lower stresses in the separator material and reduce the risk of damage.

With the created simulation model, it is now possible to investigate the influence of different gluing patterns and engagement depths of grasping jaws and identify the process and system parameters for specific battery materials and cell formats. The following step deals with the investigation of wrinkle formation by exemplary variation in the gluing pattern.

6. Step—Derive process limits through optimization | To investigate the wrinkle formation caused by the gluing dots, the adhesive is modelled as dots, lines and beads, with variation in the number of dots and lines. For the grasping jaws, a depth of engagement of 62% is used and a web tension of 4 N is applied in the simulation. The complete overview of all simulation results can be found in the Appendix A (see Figure A1). The simulation results show that for the 6 and 8 dots (patterns 2 and 3), the continuous bead (adhesive pattern 4) and the diagonal bead (adhesive pattern 7) no stresses are greater than the equivalent yield strength. With these patterns and the process and machine parameters, the ceramic separator can be processed without damage within the z-folding process for high-throughput ESC assembly.

Summary of the case study | The exemplary investigation of different gluing patterns has shown that by using simulations, interdependencies between process loads, separators and electrodes as well as machine parameters can be identified with relatively little effort. Beyond this exemplary use case, simulation-based investigations allow parameter studies

to be carried out for the optimization of processes and dimensioning parameters with the aim of overengineering-free development of machines and processes.

4. Discussion

In summary, the proposed approach can be applied to all three presented sub-process steps of ESC stacking within battery cell production. Although all processes had a different TRL, and the motivation, beginning with basic functional safeguarding up to the cycle-time optimized design, was strongly differentiated, the required results could be methodically elaborated. This demonstrates that a generic approach to the design and optimize of stacking processes was presented in this article, which can be used in different TRLs of development.

When all three case studies are considered, it becomes apparent that the individual steps of the approach were applied to a different degree of detail in each application. The approach therefore represents a recommendation for action for safeguarding and optimization and, at the same time, leaves enough room to take into account the application-specific characteristics of the process. The necessary level of detail in the individual steps of the approach results accordingly from the existing a priori knowledge about the specific sub-process step that has to be modelled.

If a low TRL is given, which was the case with the paddle wheel, only very little a priori knowledge about a specific sub-process step is available. This made it necessary, for instance, to characterize specific unknown loads such as the edge impact for the first time in order to be able to model, evaluate and classify it within the framework of the process simulation. In comparison, with a higher TRL of a further developed process step, such as the separation module, the focus falls more on the optimization of pre-existing operating resources, such as the intake module.

In all three application cases, the primary focus of the modelling was on the loads applied during handling, independent of the level of detail. For the modelling of the intermediate battery products required for this purpose, it was possible to show the characterization methods with which it is possible to map various loads on the electrode and separator and to take them into account in the design of the process. Through a process-specific characterization, it is therefore possible to model the relevant stresses caused by the process and to take them into account for subsequent process steps and/or to validate them within the framework of an electrochemical characterization.

The accuracy of the model-based process simulation can be evaluated process-specifically within the framework of the approach through intermediate validations. On the one hand, in the case of a low TRL, it is possible to determine the process-specific loads as part of the characterization of the material model with the help of material tests. On the other hand, at a higher TRL with an existing prototype of the system, it is possible to validate the process simulation exactly with the help of measurement technology and to calibrate it accordingly. For example, laser triangulation or camera-based systems can be used to compare real deformations on the intermediate product with the simulation in a sequence-related manner and to determine compensation coefficients or functions.

Within the framework of a model-based process simulation, it is therefore important to characterize a suitable material model that can represent all loads from the corresponding stacking process. With the help of this material model, the process-specific loads of the ESC intermediate products can then be reproduced, whereby the format of the ESC can be varied as desired. Furthermore, the operating resources and the performance-relevant process parameters can also be optimized on the basis of this model. However, it should be noted that novel effects contribute to an increased effort in the approach and can lead to the necessity to investigate unknown loads with the help of an electrochemical characterization of the ESC, in order to ensure the maximum acceptable load limits of the process simulation.

Depending on the development stage, it should be considered precisely when and to what extent a model-based simulation is advisable. In order to estimate the costs required to reach a targeted readiness level, reference is made to an existing publication by the

authors [50]. It shows how the economic effort of a TRL transition for a stacking process can be estimated by evaluating the TRL transition according to the value creation factors (product, process, equipment, staff and organization) according to Seliger [51].

5. Conclusions

In conclusion, it can be stated that the application of model-based process simulations enables discrete material and format machine parameters and process limits to be determined faster and more efficiently than with conventional, purely experimentally driven investigations. In addition to reducing the effort in the application, simulation-based process models contribute to achieving a high level of development safety through early validation, deriving knowledge about interactions and process understanding, to target-oriented dimensioning and, thus, to reducing the costs in the development and commissioning. In addition, model-based process simulations show the possibility of carrying out investigations without having to rely on physical products or machines, which can greatly reduce the scrap of material for the start-up and optimization of the machine. Especially in the dynamic field of battery production, where new materials and formats are constantly being introduced, the effort required for parameterization and optimization of the batch is a significant cost driver that must be minimized.

In order to keep the effort required for the development and start-up of stacking processes as low as possible, an approach was presented that was successfully applied to three examples out of current research projects. The results show that the approach can be used to design and optimize a stacking process in a simulation-based environment.

The flexibility of simulation and the broad applicability for different formats and materials, are the keys for an economic development of processes and plants as well as an economic start-up without losses due to set-up times, rejects and start-up delays. However, there are some challenges to be solved related to the application of simulation-based analysis methods in the development and commissioning of handling and joining processes of stack creation. In addition to the amount of time required, modelling and simulation needs interdisciplinary expert knowledge. The cooperation of different disciplines by utilizing the knowledge of experts from process, procedure, material, production and simulation technology enables the efficient modelling and simulation of processes in order to derive the necessary interactions for development and commissioning. From this point of view, it will be important in the future to create user-friendly software tools for developed and verified models using existing interfaces, or to integrate them into established software tools and, thus, increase their reusability.

The integration and networking of different models of battery cell production would also enable the observation and determination of interactions across process steps, and thus allow an increase in efficiency in the process chain section under consideration.

Author Contributions: Conceptualization, A.M., M.A., C.v.B. and S.R.; Funding acquisition, K.D. and F.D.; Investigation, A.M., M.A., C.v.B. and N.v.O.; Methodology, A.M., M.A. and C.v.B.; Project administration, A.M., M.A. and C.v.B.; Software, A.M., M.A. and C.v.B.; Supervision, K.D. and F.D.; Validation, A.M., M.A., C.v.B. and N.v.O.; Visualization, M.A. and C.v.B.; Writing—original draft, A.M., M.A., C.v.B., S.R. and R.L.; Writing—review and editing, A.M., M.A., C.v.B., S.R. and R.L. All authors have read and agreed to the published version of the manuscript.

Funding: This research is based on HoLiB (Reference No. 03XP0236A and 03XP0236B) and KontiBat (Reference No. 03VP01480), and was funded by the German Federal Ministry of Education and Research (BMBF). We acknowledge support by the German Research Foundation and the Open Access Publication Fund of TU Berlin.

Data Availability Statement: Part of the data presented in this study is openly available in DepositOnce at https://doi.org/10.14279/depositonce-12166, reference number [8]. Part of the data presented in this study is available on request from the corresponding author. The data are not publicly available due to ongoing study.

Conflicts of Interest: The authors declare no conflict of interest. The funders had no role in the design of the study; in the collection, analyses, or interpretation of data; in the writing of the manuscript, or in the decision to publish the results.

Appendix A

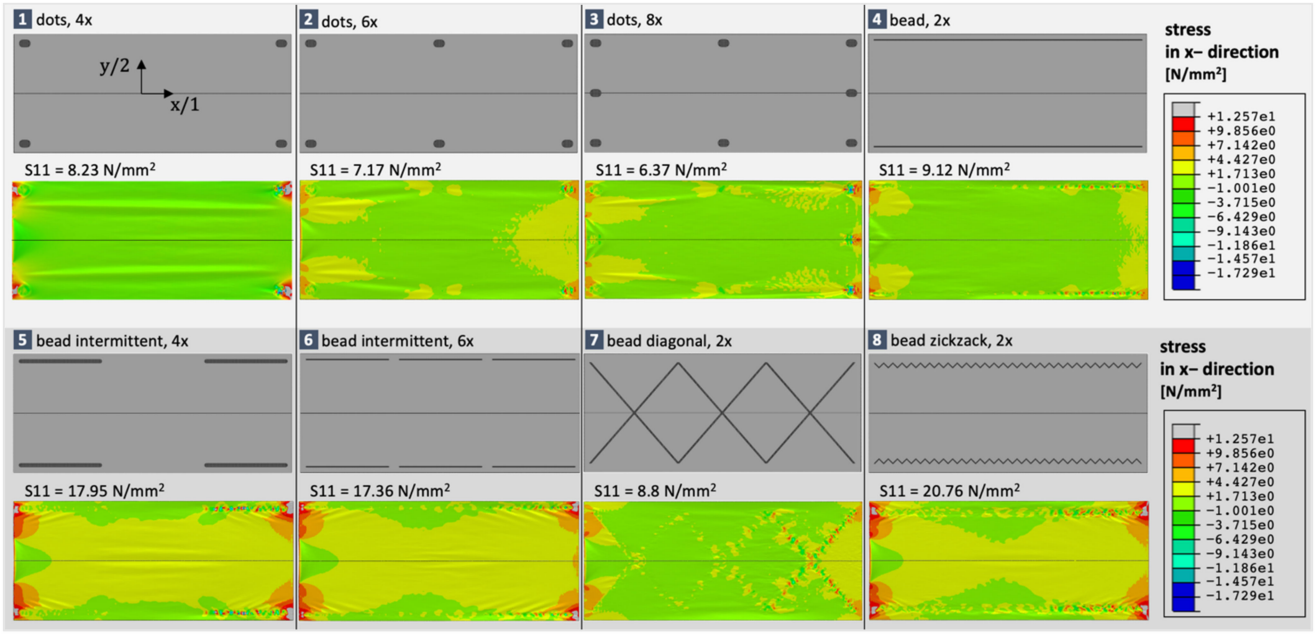

Figure A1. Normal stresses in x- and y-directions at the end of the folding motion for the ceramic separator and different web tension [8].

References

1. Forum, W.E. Global Battery Demand between 2018 and 2030, by Application (in Gigawatt Hours); Statista. Available online: https://www.statista.com/statistics/1103218/global-batterydemand-forecast (accessed on 25 October 2021).
2. Kwade, A.; Haselrieder, W.; Leithoff, R.; Modlinger, A.; Dietrich, F.; Droeder, K. Current status and challenges for automotive battery production technologies. *Nat. Energy* **2018**, *3*, 290–300. [CrossRef]
3. Schröder, R.; Aydemir, M.; Seliger, G. Comparatively assessing different shapes of lithium-ion battery cells. *Procedia Manuf.* **2017**, *8*, 104–111. [CrossRef]
4. Kampker, A. *Elektromobilproduktion*; Springer: Berlin/Heidelberg, Germany, 2014.
5. Aydemir, M.; Glodde, A.; Mooy, R.; Bach, G. Increasing productivity in assembling z-folded electrode-separator-composites for lithium-ion batteries. *CIRP Ann.* **2017**, *66*, 25–28. [CrossRef]
6. Mooy, R.J.M. Beitrag zur Produktivitätssteigerung in der Vereinzelung, Positionierung und Orientierung von Elektrodenfolien durch eine Kontinuierliche Materialbewegung. Ph.D. Thesis, Technische Universität Berlin, Berlin, Germany, 2019.
7. Bach, G. Beitrag zur Produktivitätssteigerung in der Massenherstellung von Lithium-Ionen-Batteriezellen. Ph.D. Thesis, Technische Universität Berlin, Berlin, Germany, 2017.
8. Aydemir, M. Modellbasierte Prozessgrenzenermittlung in der Entwicklung und Inbetriebnahme von Hochdurchsatz-Batteriestapelverfahren. Ph.D. Thesis, Technische Universität Berlin, Berlin, Germany, 2021.
9. Edström, K. Roadmap Battery 2030+—Inventing the Sustainable Batteries of the Future. Available online: https://battery2030.eu/digitalAssets/860/c_860904-l_1-k_roadmap-27-march.pdf (accessed on 25 October 2021).
10. Deutskens, C. Battery-News.de im Gespräch mit Prof. Dr. Fritz Klocke. Available online: https://battery-news.de/index.php/2020/03/08/prof-klocke-die-prozessablaeufe-werden-ueber-standardisierte-schnittstellen-realisiert-um-ganz-dezidiert-der-deutschen-industrie-moeglichkeiten-zu-geben-eigene-anlagentechniken-zu-entwickeln-zu/ (accessed on 25 October 2021).
11. Thiede, S.; Turetskyy, A.; Kwade, A.; Kara, S.; Herrmann, C. Data mining in battery production chains towards multi-criterial quality prediction. *CIRP Ann.* **2019**, *68*, 463–466. [CrossRef]
12. Turetskyy, A.; Thiede, S.; Thomitzek, M.; Drachenfels, N.; Pape, T.; Herrmann, C. Toward Data-Driven Applications in Lithium-Ion Battery Cell Manufacturing. *Energy Technol.* **2020**, *8*, 1900136. [CrossRef]
13. Turetskyy, A.; Wessel, J.; Herrmann, C.; Thiede, S. Data-driven cyber-physical System for Quality Gates in Lithium-ion Battery Cell Manufacturing. *Procedia CIRP* **2020**, *93*, 168–173. [CrossRef]

14. Thomitzek, M.; Schmidt, O.; Röder, F.; Krewer, U.; Herrmann, C.; Thiede, S. Simulating Process-Product Interdependencies in Battery Production Systems. *Procedia CIRP* **2018**, *72*, 346–351.
15. Brodd, R.J.; Helou, C. Cost comparison of producing high-performance Li-ion batteries in the U.S. and in China. *J. Power Sources* **2013**, *231*, 293–300.
16. Wood, D.L.; Li, J.; Daniel, C. Prospects for reducing the processing cost of lithium ion batteries. *J. Power Sources* **2015**, *275*, 234–242. [CrossRef]
17. Chinnathai, M.K.; Alkan, B.; Vera, D.; Harrison, R. Pilot to full-scale production: A battery module assembly case study. *Procedia CIRP* **2018**, *72*, 796–801. [CrossRef]
18. Brinksmeier, E.; Aurich, J.; Govekar, E.; Heinzel, C.; Hoffmeister, H.-W.; Klocke, F.; Peters, J.; Rentsch, R.; Stephenson, D.; Uhlmann, E.; et al. Advances in Modeling and Simulation of Grinding Processes. *CIRP Ann.* **2006**, *55*, 667–696.
19. Klocke, F.; Stauder, J.; Mattfeld, P.; Müller, J. Modeling of Manufacturing Technologies During Ramp-up. *Procedia CIRP* **2016**, *51*, 122–127.
20. Colledani, M.; Tolio, T.; Yemane, A. Production quality improvement during manufacturing systems ramp-up. *CIRP J. Manuf. Sci. Technol.* **2018**, *23*, 197–206. [CrossRef]
21. Zhu, J.; Wierzbicki, T.; Li, W. A review of safety-focused mechanical modeling of commercial lithium-ion batteries. *J. Power Sources* **2018**, *378*, 153–168. [CrossRef]
22. Westermeier, M. *Qualitätsorientierte Analyse Komplexer Prozessketten am Beispiel der Herstellung von Batteriezellen*; Nr. 322 in Dissertation; Forschungsberichte iwb Herbert Utz Verlag: München, Germany, 2016.
23. Weinmann, H. Influences of increasing coating thicknesses and calendering degrees on single sheet stack formation. Presented at the International Battery Production Conference (IBPC), Braunschweig, Germany, 4–6 November 2019.
24. Sangrós Giménez, C.; Finke, B.; Nowak, C.; Schilde, C.; Kwade, A. Structural and mechanical characterization of lithium-ion battery electrodes via DEM simulations. *Adv. Powder Technol.* **2018**, *29*, 2312–2321.
25. Avdeev, I.V.; Martinsen, M.J.; Francis, A.B. Materials Testing of a Lithium Ion Battery Separator for use in Finite Element Analysis. In Proceedings of the ASME 2012 International Mechanical Engineering Congress & Exposition (IMECE2012), Houston, TX, USA, 9–15 November 2012.
26. Zhu, X.; Xie, Y.; Chen, H.; Luan, W. Numerical analysis of the cyclic mechanical damage of Li-ion battery electrode and experimental validation. *Int. J. Fatigue* **2021**, *142*, 105915.
27. Kermani, G.; Sahraei, E. Review: Characterization and Modeling of the Mechanical Properties of Lithium-Ion Batteries. *Energies* **2017**, *10*, 1730. [CrossRef]
28. Schmidt, O.; Thomitzek, M.; Röder, F.; Thiede, S.; Herrmann, C.; Krewer, U. Modeling the Impact of Manufacturing Uncertainties on Lithium-Ion Batteries. *J. Electrochem. Soc.* **2020**, *167*, 060501. [CrossRef]
29. Kaiser, J.; Wenzel, V.; Nirschl, H.; Bitsch, B.; Willenbacher, N.; Baunach, M.; Schmitt, M.; Jaiser, S.; Scharfer, P.; Schabel, W. Prozess- und Produktentwicklung von Elektroden für Li-Ionen-Zellen. *Chem. Ing. Tech.* **2014**, *86*, 695–706. [CrossRef]
30. Mayer, J.K.; Almar, L.; Asylbekov, E.; Haselrieder, W.; Kwade, A.; Weber, A.; Nirschl, H. Influence of the Carbon Black Dispersing Process on the Microstructure and Performance of Li-Ion Battery Cathodes. *Energy Technol.* **2020**, *8*, 1900161. [CrossRef]
31. Schreiner, D.; Klinger, A.; Reinhart, G. Modeling of the Calendering Process for Lithium-Ion Batteries with DEM Simulation. *Procedia CIRP* **2020**, *93*, 149–155. [CrossRef]
32. Ngandjong, A.; Lombardo, T.; Primo, E.; Chouchane, M.; Shodiev, A.; Arcelus, O.; Franco, A.A. Investigating Electrode Calendering and its Impact on Electrochemical Performance by Means of a New Discrete Element Method Model: Towards a Digital Twin of Li-Ion Battery Manufacturing. *J. Power Sources* **2021**, *485*, 229320. [CrossRef]
33. Gausemeier, J.; Moehringer, S. VDI 2206-a new guideline for the design of mechatronic systems. *IFAC Proc. Vol.* **2002**, *35*, 785–790. [CrossRef]
34. Stommel, M.; Stojek, M.; Korte, W. *FEM zur Berechnung von Kunststoff-Und Elastomerbauteilen*; Hanser: München, Germany, 2018.
35. Haselrieder, W.; Westphal, B.; Bockholt, H.; Diener, A.; Höft, S.; Kwade, A. Measuring the coating adhesion strength of electrodes for lithium-ion batteries. *Int. J. Adhes. Adhes.* **2015**, *60*, 1–8. [CrossRef]
36. Bockholt, H.; Indrikova, M.; Netz, A.; Golks, F.; Kwade, A. The interaction of consecutive process steps in the manufacturing of lithium-ion battery electrodes with regard to structural and electrochemical properties. *J. Power Sources* **2016**, *325*, 140–151. [CrossRef]
37. Aydemir, M.; Müller, A.; Glodde, A.; Seliger, G. *Greifsystem für die z-Faltende Zellverbundherstellung des Elektrode-Separator-Verbunds einer Batteriezelle*; wt-Werkstattstechnik Online 108(9); Springer: Düsseldorf, Germany, 2018.
38. Von Boeselager, C.; Müller, A.; Helm, J.; Brodhun, J.; Glodde, A.; Olowinsky, A.; Leithoff, R.; Fröhlich, A.; Kandula, M.; Dietrich, F.; et al. *A Novel High-Throuput Process for the Production of Lithium Ion. Battery Cells*; wt Werkstatttechnik Online 110(9); Springer: Düsseldorf, Germany, 2020.
39. Fleischer, J.; Ruprecht, E.; Baumeister, M.; Haag, S. Automated Handling of Limp Foils in Lithium-Ion-Cell Manufacturing. In Proceedings of the 19th CIRP Conference on Life Cycle Engineering, Berkeley, CA, USA, 23–25 May 2012.
40. Hu, J.; Li, L.; Zhou, P.; Li, G.; Sun, Q. Co-simulation and Analysis of Radar Skeleton Based on ANSYS and ADAMS. In *Proceedings of the International Conference on Mechanical Design*; Springer: Singapore, 2017.
41. Li, N.; Yang, Z.; Huang, H.; Zhang, G. The dynamic simulation of robotic tool changer based on adams and ansys. In Proceedings of the International Conference on Cybernetics, Robotics and Control (CRC), Hong Kong, China, 19–26 August 2016.

42. Frimpong, S. Contact and Joint Forces Modeling and Simulation of Crawler-formation Interactions. *J. Powder Metall. Min.* **2015**, *4*, 135.
43. Zhang, G.; Xie, Q.; Zhu, S.; Zhang, Y. Flexible Multibody Dynamics of Sewing Machine with Multi-Clearance Joints. In *WCX™ 17: SAE World Congress Experience*; SAE Technical Paper Series; SAE International: Detroit, MI, USA, 2017.
44. Sapietová, A.; Gajdoš, L.; Dekýš, V.; Sapieta, M. Analysis of the Influence of Input Function Contact Parameters of the Impact Force Process in the MSC ADAMS. In *Ryszard Jabłoński und Tomas Brezina (Hg.): Advanced Mechatronics Solutions, Bd. 393*; Springer International Publishing: Cham, Switzerland, 2016.
45. Aydemir, M.; Mooy, R.; Glodde, A.; Seliger, G. Fügen von Elektrodenfolien in der Batteriezellherstellung. *ZWF Z. Wirtsch. Fabr.* **2017**, *112*, 684–689.
46. Glodde, A. Kinematische Modellierung eines Kontinuierlichen z-Faltprozesses für die Batterieproduktion. Ph.D. Dissertation, Technische Universität Berlin, Berlin, Germany, 2020.
47. Dietrich, F.; Glodde, A.; Solmaz, S. Accuracy analysis and improvement method for continuous web-based precision assembly. *CIRP Ann.* **2020**, *69*, 5–8. [CrossRef]
48. Zhang, X.; Sahraei, E.; Wang, K. Deformation and failure characteristics of four types of lithium-ion battery separators. *J. Power Sources* **2016**, *327*, 693–701. [CrossRef]
49. Hill, R. A theory of the yielding and plastic flow of anisotropic metals. *Proc. R. Soc. Lond. Ser. A Math. Phys. Sci.* **1948**, *193*, 281–297.
50. Müller, A.; Aydemir, M.; Dietrich, F. *Decision Support Based on Cost and Risk Estimation to Prioritize Battery Cell Assembly Technologies Report*; Technische Universität Berlin: Berlin, Germany, 2021.
51. Seliger, G. Sustainable manufacturing for global value creation. In *Sustainable Manufacturing*; Springer: Berlin/Heidelberg, Germany, 2012; pp. 3–8.